Prostate Gland and Extra-Capsular Tissue 3D Reconstruction and Measurement

Frederic (Rick) McKenzie, Rania Hussein, Jennifer Seevinck
Old Dominion University
Electrical and Computer Engineering Department
231-C Kaufman Hall
Norfolk, VA 23529
fmckenzi@ece.odu.edu, rhussein@odu.edu, jseevinc@odu.edu

Paul Schellhammer, Jose Diaz
Eastern Virginia Medical School
Urology and Pathology Departments
700 Olney Road
Norfolk, VA 23501
schellpf@evmsmail.evms.edu, diazji@evms.edu

Abstract

Currently there are little objective parameters that can quantify the success of one form of prostate surgical removal over another. Accordingly, at Old Dominion University (ODU) we have been developing a process resulting in the use of software algorithms to assess the coverage and depth of extra-capsular soft tissue removed with the prostate by the various surgical approaches. Parameters such as the percent of capsule that is bare of soft tissue and where present the depth and extent of coverage have been assessed. First, visualization methods and tools are developed for images of prostate slices that are provided to ODU by the Pathology Department at Eastern Virginia Medical School (EVMS). The visualization tools interpolate and present 3D models of the prostates. Measurement algorithms are then applied to determine statistics about extra-capsular tissue coverage. This paper addresses the modeling, visualization, and analysis of prostate gland tissue to aid in quantifying prostate surgery success. Particular attention is directed towards the accuracy of these measurements and is addressed in the analysis discussions.

1. Introduction

Prostate cancer continues to be the leading cancer in the United States male population. Early detection of the disease is much more common nowadays than in the past. Nevertheless, surgical removal still remains the standard procedure for cure. Currently there are little objective parameters that are used to compare the efficiency of one form of surgical removal or another. As surgeons apply different approaches of surgical removal, a quality of assurance assessment would be most useful, not only with regard to overall comparison of one approach versus another but also to surgeon evaluation of personal results as they relate to a standard.

In order to computerize and quantify the assessment process, it is essential to have a 3D reconstructed model for the prostate gland. With such a model, the curvature of the gland, the irregular borders of the extra-capsular tissues as well as the extensions of the tumor can be visualized. In general, the reconstruction process consists of three main steps: a) extracting the object contours, b) interpolating intermediate contours, and c) reconstructing surfaces or volumes. During the last decade, there has been a considerable amount of research in the visualization and the 3D reconstruction of medical data. Most research focused on developing or improving algorithms that consider the last two steps of the reconstruction process.

For example, Xuan (1998) developed an elastic contour model to perform nonlinear interpolation between a start contour of a prostate gland and a goal contour. The 3D prostate model was reconstructed from the interpolated contours by applying external forces to a dynamic deformable surface spine model controlled by a second order partial differential equation from Lagrangian mechanics. Tanaka & Kishino (1993) introduced a surface

reconstruction model based on Meusnior theorem from differential geometry by which the arbitrary view of the object surfaces can be reconstructed. A number of control points are generated according to the view direction, where the shape at these points is recovered from the shape description in their neighborhood. Using this theorem, the curvature of a cross section of the surface with planes parallel to the view direction can be recovered. Xu et al described a fuzzy segmentation algorithm to obtain a surface representation of the central layer of the human cerebral cortex from MR images. However this system suffers from several problems regarding the intensity inhomogeneities of the images, and the convergence of the deformable model to boundary concavities. This algorithm was improved in [4] where a more robust algorithm was used to solve these problems. Rader et al described the 3D reconstruction of a human heart fascicle by using PC-based tools (SurfDriver). This work was not an algorithm for reconstruction and is highly dependent on the judgments of the anatomist. The measurements of the size and orientation of fascicles in 3D which were measured in this paper was determined by some features of the software used.

The reconstruction phase may be regarded as the first step towards quantifying the 3D models. The authors of [6] compared the prostate gland deformations that occur between pretreatment MR imaging and intraoperative MR imaging during brachytherapy. They measured dimensions like the greatest transverse dimension of the gland, as well as the total dimension of the gland. However, these measurements were defined manually with the 3D slicer software used. Other researchers obtained the quantity information from 2D slices taken from 3D images [7].

The objective of this research is to develop a process resulting in the use of software algorithms to assess the percentage and depth of extra-capsular soft tissue removed with the prostate by the various surgical approaches. Measurement and visualization methods and tools have been developed for images of prostate slices provided to Old Dominion University by the Pathology Department at Eastern Virginia Medical School (EVMS). Analysis performed on test images has led to a procedure to accurately measure the percentage of extra-capsular soft tissue coverage. The final goal of this assessment will be to collect a statistically significant number of prostate images, reconstruct and analyze them using the procedures already developed, visualize this data, and permit the pathologist and the surgeon to make an assessment of the adequacy/appropriateness of surgical approaches; laparoscopic versus open perinea or retro-pubic prostatectomy.

2. Preparing Prostate Slices

The test images provided were taken from traditionally processed prostate slices where a pathologist would simply slice the prostate at imprecise intervals and place these slices on microscope slides primarily to assess the presence of cancer. Normal microscope slides are to narrow for a whole mount of the prostate slice; therefore, these slices are further divided so that they may fit on the microscope slides. As a result, after image capture, each prostate slice image consists of about four to six parts that are combined to form one slice. This process of preparation has its limitations due to the possibility of tissue shrinking or deformation. It is also possible that the slices may be flipped while placed on the microscope slides or while scanned. The results reported in this paper are based on this traditional method. Indeed this is the worst-case scenario.

Currently, a new protocol is being used which should enhance the appearance and preparation of the slices and hence improve the results. In this new process, the specimen is received fresh. The whole gland is inked blue on the right and black on the left to label the surgical margins so any flipping is avoided. The gland is then cut transversally from apex to base. The first section is cut 6 mm thick and contains the apex. The remainder of the gland is cut transversally at 3 mm intervals from apex to base; this makes the reconstruction phase more accurate since the distance between the slices is well defined. To facilitate accurate cutting of the fresh gland, the gland is caste with alginate in a cubical chamber and the gel containing the gland is sectioned with an electrical tissue slicer for whole mount processing and tumor banking, so any shrinking or deformation is minimized. This process will be used in future experiments.

3. Prostate Modeling Process

The initial data consists of a series of nine cross-sectional slices prepared by the traditional method of slicing described in section 2. The contours needed to reconstruct the model are the outer edges of the extra capsular tissue and the prostate gland boundary which was manually drawn as a yellow line placed on a separate layer to the slices (see Figure 1).

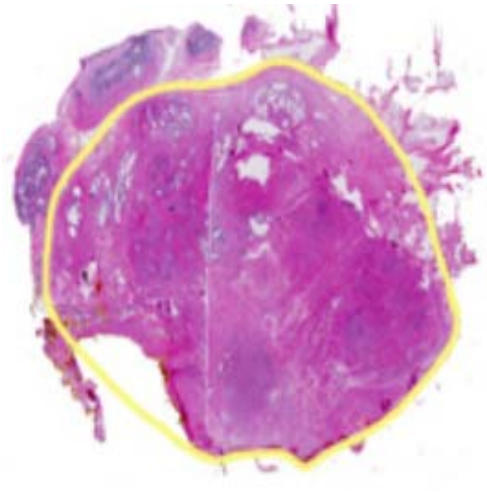

Figure 1. A prostate slice with the hand-drawn yellow boundary

The hand drawn yellow gland boundary as it currently stands has 2 edges, an inside edge of the pen line and an outside edge. The Pen line width is approx .046 inches or 1.1 mm. Furthermore, these edges are aliased, or blurred. Each of The contours was preprocessed in the Photoshop software package and a single, clean edge is obtained to generate the required curve. The inside edge of this hand-drawn gland boundary line is assumed to be the gland and it is assumed that there is no capsule underneath this line. The fat boundary contours were taken as the continuous perimeter of the outer surface of the scanned prostate slices. Nine contours were generated this way and are separated from the capsular contours.

Each slice's image file is manipulated to create 2 additional files, one conveys the gland boundary information and the other conveys the fat boundary information. These files are then read into a 3D modeling package to extrapolate a geometric curve. The series of curves derived from all the slices' images are skinned and lofted together to reconstruct a 3D model of the prostate (Figure 2a). The distance between the consecutive polygonal curves is arbitrarily decided to be of approximately 5.33 mm. In the last stage of the reconstruction phase, a triangular, polygonal mesh surface is interpolated between the consecutive slices of the extra-capsular tissue curves, resulting in a gland model and a fat model. After reconstructing the meshes, a point cloud bounded by the reconstructed meshes is generated for each of the gland and the fat models (Figure 2b).

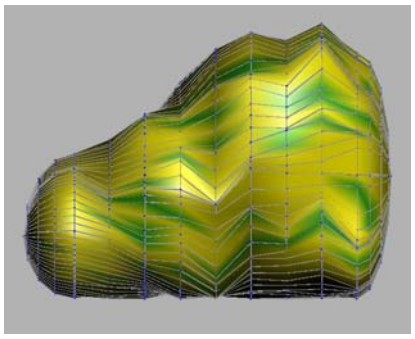

(a)

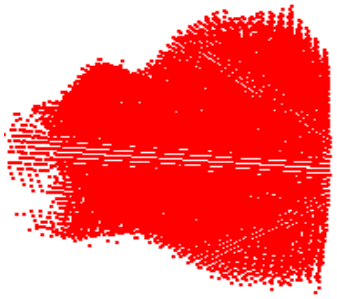

(b)

Figure 2. (a) A skinned model of a prostate gland, (b) a generated point cloud for a prostate gland

4. Calculating the percentage of coverage

Two separate files were generated to represent both the gland and fat models. The files which contained the point cloud information were saved in an .OBJ file format. Each of these OBJ files was read into a separate matrix and then mapped to one 3D matrix. The location of each point in the gland matrix was mapped to its corresponding point in the 3D matrix by the following equations

xloc = (a.x/1.2)*xsize + xoffset
xoffset = morenegX *xsize

yloc = (a.y/1.2)*ysize + yoffset
yoffset = morenegY *ysize

zloc = (a.z/2.4)*zsize + zoffset
zoffset = morenegZ *zsize

Where

Xloc,yloc,zloc are the x,y,z coordinates of the 3D matrix,

a.x,a.y,a.z are the value of the x,y,z coordinates of the current point in the gland matrix,

xsize,ysize,zsize are the maximum size of the 3D matrix in the x,y,z-directions (it was chosen to be 50,50,100 respectively, or 100,100,200 for the denser point cloud model)

morenegX, morenegY, morenegZ are the absolute value of the greatest negative value of the minimum value in the x,y,z-directions. They were chosen to be 0.5, 0.5, and 0 respectively.

The values of 1.2,1.2, 2.4 are the length of the model in Houdini units in the x,y,z-directions respectively.

Once the location of the current point is calculated, a value of '1' is assigned to that location of the matrix as long as the current point represents a gland point. After mapping the gland points, the fat points were mapped by the same techniques. However, value '2' was assigned to the calculated fat location if this location was not occupied by a gland point otherwise a value of '3' is assigned. The 3D matrix is scanned until a point on the surface of the gland is encountered. Subsequently, a Von Neuman neighborhood check for fat points is performed. Fat points encountered in this manner will increase the count of covered gland points while also contributing to the total number of gland points encountered (covered or uncovered). The ratio of these counts provides the percentage of extra-capsular tissue coverage for a particular prostate.

5. Results

The results can be summarized in the table below.

	Model constructed using 50*50*100 divisions	Denser point cloud using 100*100*200 divisions
# Of original gland points	15882	126187
# Of original fat points	19699	155948
# Of gland points after mapping	3385	28946
# Of fat points after mapping	6975	57504
# Of gland and fat points mapped to the same location	11538	93527
# Of gland points on the prostate surface	1768	7922
# Of gland points covered (by checking the 8 neighbors of the point)	1420	6079
% Coverage (by checking the 8 neighbors of the point)	80.3167	76.7357

6. Error analysis

In this section, errors that can occur at any of the three phases of our process are discussed.

6.1 During data preparation

Using the traditional way of cutting the prostates, some errors can occur during the preparation and hence appear in the scanned slices. The slices may be flipped or they may be upside down and during cutting, the gland may shrink or deform due to its elasticity

The new method described in section 2 should eliminate the possibility that a slice was flipped when scanned. And once the urethra is clear, the problem of an upside down slice should vanish. Elasticity of the gland should also be greatly reduced due to the alginate cast.

6.2 During reconstruction

During the reconstruction phase, a number of issues are of concern. Firstly, the thickness of the hand drawn line is an issue since its inner edge is used to construct the model. The thickness of the line is approximately 0.046 inches thick. The fact that is manually drawn is a source of error. The thickness makes deciding whether to consider its inner or outer edge an issue. If the inside edge is considered, then the boundary that separates the gland from the fat tissue (capsule) might be under-estimated, while considering its outer edge might over estimate the capsule. It is believed that this error would contribute in the worst case to the calculation of the fat tissue average thickness measurement by the thickness of the line plus the longest distance between point cloud points (.046 + .0523= .0983).

Developing an algorithm to automatically determine the capsule can solve this problem. This algorithm will require that the slices be scanned at a very high resolution to be able to recognize the wavy pattern of the gland that constructs the capsule. In the mean time, the resolution is not an issue in our results since the capsule is pre-determined manually.

Secondly, due to the fact that the scanned images were not clear enough to show the urethra around which the slices should be aligned, the slices were aligned on the same level as the bottom of the first slice. The slices should be aligned around the urethra as well as on the level of the posterior side. Nevertheless, the urethra is not clear enough at the current resolution, so the slices were only aligned on the posterior level and centered otherwise with an inter-slice distance of 0.218 inches (0.1 Houdini units). This chosen distance between slices is also a source of error since care was not taken in the test slices to measure this distance. In the new protocol, the slices will be made equidistantly. The distance that will be between each slice will be 3 millimeters (≅ 0.12 inches)

6.3 Accuracy of percentage of coverage calculation

In the mapping phase, the number of points in the 3D matrix is less than the number of the vertices generated in the reconstruction phase. This is due to the fact that using the mapping equations, more than one point can be mapped to the same location. Approximately, 6% of points map to the same point in the 50x50x100 map while that number drops to about 3% in the denser mapping. This is thought to be negligible and due to round off error. A more telling issue is the density of the point clouds themselves. It is believed that point cloud density contributes to error in the percentage of coverage by affecting points on the perimeters of the uncovered areas. These points may differ in the worst-case scenario by the hypotenuse of adjacent points. The density of the 50x50x100 model is 6982.265 points/in^3 where points are .0523 inches apart. Therefore, the hypotenuse is .074 inches. This indicates that in the worst-case scenario, covered points would differ by the total of all the perimeters divided by .074. In the case of the denser point cloud (55,858.12 points/ in^3), points are .02616 inches apart and the hypotenuse is .037 inches making the worst-case here to be total of perimeters divided by .037.

7. Summary and Future work

This paper introduces a process resulting in the use of software algorithms to assess the percentage and depth of extra-capsular soft tissue removed with the prostate by the various surgical approaches. Results obtained were based on traditional protocols in preparing prostate pathology; the accuracy of this measurement is dependent upon possible errors such as shrinkage and tissue deformation. It is expected that the new protocol will eliminate significant effects from these errors. However, some error is introduced in the density of the point cloud and the 3D matrix mapping. In future work, the same method will be performed on a new set of images prepared by the new protocol, as well as developing a mathematical prostate model and initializing its parameters with real measurements from actual prostate slices so that more accurate measurements can be obtained.

8. References

[1] Xuan, J. Sesterhenn I., HayesWS,Wang Y., Adali T., Yagi Y, Freedman M.T, Mun S.K. (1998). "Surface Reconstruction and Visualization of the surgical prostate model" *Proceedings of the SPIE Medical Imaging Conference*, 1997, 3031: 50–61.

[2] Hiromi T. Tanaka, Fumio Kishino, "Surface reconstruction model for realistic visualization," IEICE transactions on information and systems, vol. E76-D No. 4, 1993.

[3] C.Xu, D.L.Pham, and J.L.Prince. "Finding the brain cortex using fuzzy segmentation isosurfaces, and deformable surface models." In the XVth *International Conference on Information Processing in Medical Imaging* (IPMI), pages 399-404. Springer-Verlag, 1997.

[4] C. Xu, D. L. Pham, M. E. Etemad, D. N. Yu, and J. L. Prince, "Reconstruction of the Central Layer of the Human Cerebral Cortex from MR images**,**" in *Proc. of the First International Conference on Medical Image Computing and Computer Assisted Interventions (MICCAI'98)*, pp. 482-488, 1998

[5] Rader, Robert J., Phillips, Steven J., LaFollette, Paul S., and Temple Univ. Medical School, 3D reconstruction of a human heart fascicle using SurfDriver**,** Proc. SPIE Vol. 3979, p. 609-617, Medical Imaging 2000: Image Processing, Kenneth M. Hanson; Ed.

[6] Hirose M, Bharatha A, Hata N, Warfield SK, Zou KH, Cormack, RA, D'Amico A, Kikinis R, Jolesz FA, Tempany CMC, ″Quantitative MRI Assessment of Prostate Gland Deformation Before and During MR-guided Brachytherapy″ – Journal of academic Radiology, vol. 9, No. 8, August 2002.

[7] S. Solloway, C.J. Taylor, C.E. Hutchinson and J.C. Waterton, "Quantification of Articular Cartilage from MR Images Using Active Shape Models," Proceedings of the 4th European Conference on Computer Vision, Cambridge University, 1996, pp. 400-412.